

**Title: A seasonal agricultural drought forecast system for food-insecure regions of East Africa**

**Authors:** Shraddhanand Shukla<sup>1,2</sup>, Amy McNally<sup>1,4,5</sup>, Greg Husak<sup>1</sup> and Christopher Funk<sup>1,3</sup>

<sup>1</sup> Climate Hazards Group, Department of Geography, University of California, Santa Barbara, CA, USA.

<sup>2</sup> University Corporation for Atmospheric Research, Boulder, CO, USA.

<sup>3</sup> U.S. Geological Survey, USA.

<sup>4</sup> Earth System Science Interdisciplinary Center, University of Maryland, College Park, MD, USA.

<sup>5</sup> Hydrological Sciences Laboratory, NASA Goddard Space Flight Center, Greenbelt, MD, USA.

**Corresponding author:** Shraddhanand Shukla (shrad@geog.ucsb.edu)

## Abstract

1  
2 The increasing food and water demands of East Africa's growing population are stressing  
3 the region's inconsistent water resources and rain-fed agriculture. More accurate seasonal  
4 agricultural drought forecasts for this region can inform better water and agro-pastoral  
5 management decisions, support optimal allocation of the region's water resources, and mitigate  
6 socio-economic losses incurred by droughts and floods. Here we describe the development and  
7 implementation of a seasonal agricultural drought forecast system for East Africa (EA) that  
8 provides decision support for the Famine Early Warning Systems Network's (FEWS NET)  
9 science team. We evaluate this forecast system for a region of equatorial EA ( $2^{\circ}$  S to  $8^{\circ}$  N, and  
10  $36^{\circ}$  to  $46^{\circ}$  E) for the March-April-May growing season. This domain encompasses one of the  
11 most food insecure, climatically variable, and socio-economically vulnerable regions in EA, and  
12 potentially the world; this region has experienced famine as recently as 2011.

13 To produce an 'agricultural outlook', our forecast system simulates soil moisture (SM)  
14 scenarios using the Variable Infiltration Capacity (VIC) hydrologic model forced with climate  
15 scenarios describing the upcoming season. First, we forced the VIC model with high quality  
16 atmospheric observations to produce baseline soil moisture (SM) estimates (here after referred as  
17 SM a posteriori estimates). These compared favorably (correlation=0.75) with Water Required  
18 Satisfaction Index (WRSI), an index that the FEWS NET uses to estimate crop yields. Next, we  
19 evaluated the SM forecasts generated by this system on March 5<sup>th</sup> and April 5<sup>th</sup> of each year  
20 between 1993-2012 by comparing them with corresponding SM a posteriori estimates. We found  
21 that initializing SM forecasts with start-of-season (SOS) (March 5<sup>th</sup>) SM conditions resulted in  
22 useful SM forecast skill (>0.5 correlation) at 1-month, and in some cases 3-month, lead times.  
23 Similarly, when the forecast was initialized with mid-season (i.e. April 5<sup>th</sup>) SM conditions, the

24 skill of forecasting SM estimates until the end-of-season improved (correlation  $>0.5$  over several  
25 grid cells). We also found these SM forecasts to be more skillful than the ones generated using  
26 the Ensemble Streamflow Prediction (ESP) method, which derives its hydrologic forecast skill  
27 solely from the knowledge of the initial hydrologic conditions. Finally, we show that, in terms of  
28 forecasting spatial patterns of SM anomalies, the skill of this agricultural drought forecast system  
29 is generally greater ( $>0.8$  correlation) during drought years (when standardized anomaly of  
30 MAM precipitation is below 0). This indicates that this system might be particularly useful for  
31 identifying drought events in this region and can support decision making for mitigation or  
32 humanitarian assistance.

33

34

35 **1. Introduction**

36 The 2011 famine in the Horn of Africa was one of the most severe humanitarian disasters of  
37 this century. It affected more than 13 million people (Hillier, 2012) and resulted in a disastrous  
38 loss of life. According to Food and Agriculture Organization (FAO) and FEWS NET reports,  
39 there were between 244,000 to 273,000 famine related deaths in southern and central Somalia  
40 alone (Checchi and Robinson, 2013). While the situation was most dire in this region (Mosley,  
41 2012), the impacts spilled over the border into south-eastern Ethiopia and northern Kenya. To  
42 mitigate socio-economic losses of future drought events of this magnitude timely and adequate  
43 responses to drought early warnings are crucial (Hillier, 2012).

44 FEWS NET is a program of the United States Agency for International  
45 Development (USAID) tasked with providing timely and rigorous early warning and  
46 vulnerability information on emerging and evolving food security issues. FEWS NET is active in  
47 more than 30 of the world's most food-insecure countries including Ethiopia, Kenya, and  
48 Somalia. Each month FEWS NET's regional food analysts compile a set of agroclimatic working  
49 assumptions (i.e. hypotheses) for the upcoming season. Meanwhile FEWS NET's hydroclimate  
50 scientists review those assumptions with a deeper focus on the climate conditions and contribute  
51 to the assumptions if need be. This process requires compiling available information on soil  
52 moisture (SM), rainfall, vegetation health, sea surface temperatures (SSTs) and temperatures  
53 (land surface and air) to provide weekly-to-seasonal climate outlooks.

54 Thus far, the hydroclimate science team has focused on forecasting rainfall anomalies of  
55 the upcoming season, as well as real-time monitoring and attribution activities (Funk et al., 2005,  
56 2010). Due to this attention, rainfall estimation has also experienced significant technical  
57 advances and is the premier input to assess agricultural production and available water resources

58 (Funk et al., 2014b). While seasonal rainfall may be the most accessible indicator of yields, we  
59 argue that future attention needs to be shifted toward monitoring and forecasting of SM. Rainfall  
60 indicates meteorological drought, whereas SM in cropping zones during the growing season is a  
61 more direct indicator of agricultural drought. Furthermore, accurate SM initialization  
62 significantly contributes to the forecast skill of available moisture for up to six months (Koster et  
63 al., 2010; Shukla and Lettenmaier, 2011; Shukla et al., 2013). Due to the shortage of real time  
64 observed SM measurements, estimates computed using hydrologic models are among the best  
65 indicator of antecedent SM conditions and agricultural drought (Keyantash and Dracup, 2002).  
66 These same hydrologic models can be driven with climate forecasts for the upcoming season to  
67 provide SM forecasts. This additional step of using forecast rainfall and other meteorological  
68 variables to provide a seasonal outlook for plant available water provides a more nuanced and  
69 accurate assessment of agricultural drought conditions than rainfall forecasts alone. We show  
70 here that the combination of rainfall observations and forecasts produces more accurate SM  
71 predictions.

72         During the October-November-December growing season of 2013, the FEWS NET  
73 science team developed and implemented a seasonal agricultural drought forecast system using  
74 the Variable Infiltration Capacity (VIC) hydrologic model and National Centers of  
75 Environmental Prediction's (NCEP) Climate Forecasts System Version-2 (CFSv2). This system  
76 produces SM forecasts that are used for providing agricultural drought assessment. The primary  
77 objective of this manuscript is to describe the development and evaluation of the SM forecasts  
78 generated by the seasonal drought forecast system. Although the intended domain of this system  
79 expands over the Greater Horn of Africa, we focus on the equatorial East Africa (EA) (i.e.  
80 southeastern Ethiopia, northern Kenya, and southern Ethiopia as captured in Fig. 1) as a test-bed.

81 This region is predominantly a pastoral area with some crop zones. For evaluation of this system  
82 we chose to focus on March-April-May (MAM), which is the primary growing and rainy season  
83 as shown by the ratio of MAM and annual precipitation based on the Climate Hazards Group  
84 InfraRed Precipitation with Station data (CHIRPS) dataset (Funk et al., 2014b) (see section 2.2)  
85 in Fig. 1.

86         Reliable rainfall forecasts at a seasonal scale over this region during the rainy season  
87 have proven to be a challenge (Nicholson, 2014; Owiti et al., 2008). However, retrospective  
88 analysis shows us that rainfall in MAM season has declined in last two decades (Funk et al.,  
89 2008; Lyon and DeWitt, 2012; Williams and Funk, 2011). Although the primary causes of this  
90 decline has been a matter of debate (Hoell and Funk, 2013a; Lyon and DeWitt, 2012; Tierney et  
91 al., 2013), it seems likely that both anthropogenic warming and decadal variability have  
92 contributed to more frequent droughts, but in ways that may be making rainfall more predictable  
93 (Funk et al., 2014a and Funk et al. 2013). In the future, the MAM season will continue to be  
94 prone to drought events and continue to pose challenges for water and drought management,  
95 given increases in population and water demands as well as degradation of land in the past few  
96 decades (Pricope et al., 2013). These facts support a need to improve and develop tools to assist  
97 decision makers.

98         In the remainder of this manuscript we describe the approach and data used to implement  
99 the agricultural drought forecasts system, its evaluation, and future directions.

## 100         **2. Approach and Data**

101         This section describes the approach undertaken to develop the seasonal agricultural drought  
102 forecast system. Our approach is similar to other experimental/operational seasonal hydrologic  
103 and drought forecast systems including the NCEP's Multimodal Drought Monitoring System

104 (<http://www.emc.ncep.noaa.gov/mmb/nldas/drought/>), the Climate Prediction Center's Land  
105 Surface Monitoring and Prediction System  
106 ([http://www.cpc.ncep.noaa.gov/products/Soilmst\\_Monitoring/US/Soilmst/Soilmst.shtml](http://www.cpc.ncep.noaa.gov/products/Soilmst_Monitoring/US/Soilmst/Soilmst.shtml)), as well  
107 as Princeton University's Africa Flood and Drought Monitor  
108 (<http://stream.princeton.edu/AWCM/WEBPAGE/index.php>) (Sheffield et al., 2013) and  
109 Contiguous United States (CONUS) seasonal drought forecasting system  
110 (<http://hydrology.princeton.edu/forecast/current.php>) (Yuan et al., 2013b).

111 We used the same model parameters and temperature and wind forcings as these systems;  
112 however, we used different precipitation and a different approach for generating seasonal climate  
113 scenarios. More specifically, the CHIRPS rainfall dataset blends in more station data than other  
114 products and uses a high resolution background climatology, providing better estimates of  
115 precipitation means and variations, resulting in a better hydrologic state. The seasonal climate  
116 scenarios are based on a statistical-dynamical downscaling approach that leverages the strengths  
117 of global forecast systems. A schematic diagram shown in Fig. 2 summarizes our approach and  
118 lists all the data and models used to implement this system.

119 In following sections we describe in detail the hydrology model (section 2.1), observed  
120 atmospheric forcings (section 2.2), and the methodology adopted to build seasonal climate  
121 scenarios (section 2.3) and generate seasonal forecasts of SM (section 2.4).

## 122 **2.1 Hydrologic Model and Parameters**

123 For this analysis we used the VIC model, which is a semi-distributed macroscale  
124 hydrology model. The VIC model has been widely used at global scale and has been

125 demonstrated to accurately capture the hydrology of different regimes (Nijssen et al., 1997,  
126 2001; Maurer et al., 2002; Adam et al., 2007).

127         The VIC model parameterizes major surface, subsurface, and land-atmosphere  
128 hydrometeorological processes (Liang et al., 1994, 1996; Nijssen et al., 1997) and represents the  
129 influence of sub-grid spatial heterogeneity (in SM, elevation, and vegetation) on runoff  
130 generation. The VIC model uses the University of Maryland land cover classification system to  
131 assign different vegetation types (and bare soil) to each grid cell. Actual evapotranspiration in  
132 the VIC model is calculated using the Penman-Monteith equation. Total actual  
133 evapotranspiration is the sum of transpiration and canopy and bare soil evaporation, weighted by  
134 the land cover fraction within each grid cell. The soil profile (i.e. depth) in the VIC model is  
135 partitioned into three layers. The first layer has a fixed depth of 10 cm and responds quickly to  
136 changes in surface conditions and precipitation, while the lower layers characterize slower,  
137 seasonal SM behavior. Moisture transfers between the first and second, and second and third soil  
138 layers are governed by gravity drainage, with diffusion from the second to the upper layer  
139 allowed in unsaturated conditions (Liang et al., 1996). Baseflow is a non-linear function of the  
140 moisture content of the third soil-layer (Todini, 1996).

141         The soil and vegetation parameters used for this study were originally developed for  
142 Princeton's Africa Flood and Drought Monitor  
143 ([http://hydrology.princeton.edu/~nchaney/ADM\\_ML/](http://hydrology.princeton.edu/~nchaney/ADM_ML/)), documented in Sheffield et al. (2013) and  
144 Chaney et al (2013). For a complete list of the soil parameters used by the VIC model see:  
145 <http://www.hydro.washington.edu/Lettenmaier/Models/VIC/Documentation/SoilParam.shtml>).  
146 We briefly describe their origin and sources here for the benefit of the reader. Soil texture and  
147 bulk density were from Batjes (1997) and the rest of the soil parameters were from Cosby et al.



148 (1984). In order to insure that the VIC model yields reasonable water balance, the soil  
149 parameters were calibrated, following the method of Troy et al. (2008), against runoff fields  
150 derived by Global Runoff Data Center gauges in Africa. Troy et al. (2008) demonstrated that this  
151 approach is sufficiently accurate, computationally efficient, and results in reasonable soil  
152 parameters for ungauged basins, which makes it particularly attractive for a data sparse region  
153 such as Africa. Vegetation parameters were taken from Nijssen et al. (2001b), where each  
154 vegetation type has specific root length, minimum stomatal resistance, architectural resistance,  
155 roughness length, and displacement length. Leaf Area Index (LAI) and albedo vary monthly.  
156 Monthly LAI values used in this study were derived from Myneni et al. (1997).

## 157 **2.2 Observed atmospheric forcings**

158 This project used the CHIRPS rainfall product (Funk et al. 2014), which is available from  
159 1981-near present. This dataset was developed and is updated at near-real time by the United  
160 States Geological Survey (USGS) in collaboration with the Climate Hazards Group of the  
161 Department of Geography at the University of California, Santa Barbara. CHIRPS is generated  
162 by blending together three different datasets: (1) global 0.05° precipitation climatology (2) time  
163 varying grids of satellite based and climate model precipitation estimates, and (3) in situ  
164 precipitation observations. This dataset has been compared with other global precipitation  
165 datasets such as Global Precipitation Climatology Project (GPCP), and has a high level  
166 agreement in our area of interest.

167 Other meteorological inputs include maximum and minimum daily temperature and wind  
168 speed. From 1982-2008 we used the data described in Chaney et al. (2013) and Sheffield et al.  
169 (2006, 2013). From 2009 to present we used Global Ensembles Forecast System (GEFS) (Hamill

170 et al., 2013) temperature (daily Tmax and Tmin) analysis fields (accessed from:  
171 <http://www.esrl.noaa.gov/psd/forecasts/reforecast2/download.html>). For a continuous record, we  
172 bias-corrected these data relative to the previous time period using a quantile-quantile mapping  
173 approach for the overlapping climatological period of both dataset (i.e. 1985-2008). For the wind  
174 speed post-2009 we used the climatological monthly mean of wind speed data over 1982-2008.  
175 Livneh et al. (2013) demonstrated that using climatological mean value of wind speed has  
176 minimal impact on simulated SM.

### 177 **2.3 Seasonal Climate Scenarios**

178 In order to generate SM forecasts with the VIC model, we needed scenarios of gridded  
179 daily precipitation and temperature for the upcoming season. The conventional approach is to  
180 downscale (both spatially and temporally) seasonal climate forecasts generated by dynamical  
181 models (Wood et al., 2002; Yuan et al., 2013b). However, dynamical precipitation forecasts for  
182 EA have very limited forecast skill ( $r < 0.3$ ), especially during the main boreal spring growing  
183 season (Yuan et al., 2013b). Instead, we generated seasonal scale climate scenarios by using the  
184 hybrid dynamical-statistical downscaling approach described here.

185 Our novel approach uses an ensemble mean of the 1993-2012 CFSv2 MAM seasonal  
186 precipitation forecasts over Indo-Pacific ocean region to generate climate scenarios over the EA  
187 domain. We used the CFSv2 forecasts over Indo-Pacific domain because (1) there is a strong  
188 teleconnection between precipitation over Indo-Pacific region and EA rainfall during the MAM  
189 season and (2) dynamic forecast models have higher skill of over the Indo-Pacific ocean region  
190 than over terrestrial regions of EA. We limit our period of analysis for both generating climate  
191 scenarios and SM forecasts to 1993-2012 based on Funk et al. (2013), which reported that the  
192 teleconnection between MAM rainfall over the EA region (Fig. 1) and Indo-Pacific SST has

193 been the strongest since 1993. This increase in sensitivity can at least partially be attributed to  
194 the co-occurrence of La Niña events with a strong West Pacific Gradient (WPG) (Hoell and  
195 Funk, 2013b). Funk et al. (2014a) revisits the empirical relationship between EA rainfall and the  
196 WPG; that heuristic paper supports the more rigorous analysis provided here.

197 In brief, our approach of generating seasonal climate scenarios involved first estimating  
198 the similarity between the target year precipitation forecasts with climatological years (i.e. 1993-  
199 2012, except the target years itself). Next, based on the similarity, we generated weights to guide  
200 a simple bootstrapping process of selection of atmospheric forcings (precipitation, temperature  
201 maximum, temperature minimum, and wind speed) from the climatological years (i.e. 1993-2012  
202 except the target year) to generate scenarios of daily weather patterns for the target season (i.e.  
203 seasonal climate scenarios). The specific steps undertaken to generate seasonal climate scenarios  
204 are as follows:

#### 205 **A. Estimating Weights**

- 206 1. We first calculate the correlation between the standardized anomaly of MAM observed  
207 rainfall (CHIRPS) time series averaged for the EA study region (Fig. 1) with the  
208 standardized anomaly of CFSv2 precipitation forecasts at each grid cell over the entire  
209 globe. The period of 1982-2012 is used to standardize both datasets and the correlation is  
210 calculated over 1993-2012. Areas of highest correlation ( $[r]>0.35$ ), within the domain  
211 shown in Fig. 3 (hereafter refereed as analog domain), are used to calculate similarities  
212 between the target year and hindcast years (1993-2012) as described in steps 2-3.
- 213 2. We then multiply the standardized anomaly of CFSv2 forecasts of all hindcast years  
214 (1993-2012) over the analog domain by the absolute value of the correlation values (as

215 discussed in step 1). Using the absolute correlation value allows us to put less weight on,  
216 or effectively discard, the CFSv2 forecasts for those grid cells in the analog domain that  
217 demonstrate little correlation (negative or positive) with MAM rainfall in the EA study  
218 region.

219 3. Next, we estimate the first principal component of correlation scaled CFSv2 precipitation  
220 forecasts (as in step 2) and regress that against the observed MAM precipitation of EA  
221 domain. This results in hindcast estimates (over 1993-2012) of MAM precipitation over  
222 the EA region. We then calculate the distance (i.e. squared difference) between hindcast  
223 estimates for any given target year CFSv2 forecasts with the observed precipitation of all  
224 hindcast years (1993-2012), except the target year itself. The inverse of these distances  
225 are used to produce final weights for sampling daily seasonal climate scenarios for a  
226 given target year as described in step 4 to 6.

227 4. The final weights for sampling daily scenarios are then generated using the inverse of  
228 distances as in step 4, referred to as “ $W_i$ ” and a set of equiprobable climatological  
229 weights (i.e. 1/number of years) “ $W_{\text{clim}}$ ”. The blending of weights to generate final  
230 weights is done based on skill “ $s$ ” of hindcast estimates of precipitation (i.e. the  
231 correlation between the hindcast estimates as mentioned in step 3 and observed  
232 precipitation) as shown in equation (1):

$$233 \quad W_f = sW_i + (1 - s)W_{\text{clim}} \quad (1)$$

234 Hence in the case of  $s=0$  for any given season, our approach will simply yield  $W_f = W_{\text{clim}}$ ,  
235 resulting in climatological forecasts, whereas the higher the skill “ $s$ ”, the more  $W_f$  will  
236 be closer to  $W_i$ .

237 This weighting scheme allows us to include all available years in the climatological  
238 period (consisting of each year between 1993-2012, except the target year), although at a  
239 reduced likelihood, for generating climate scenarios (in contrast to the “constructed analog”  
240 approach suggested by Hidalgo et al. (2008) which only relies on a few best analogs).

## 241 **B. Generating Daily Scenarios**

- 242 5. To generate daily climate scenarios we start with the final weights  $W_f$  mentioned in step  
243 4. We use these weights to guide the probability of selection during the bootstrapping  
244 process (following the methods described in Husak et al., 2013) from the observed MAM  
245 precipitation over the EA domain during the hindcast years (1993-2012). The years with  
246 higher weights get selected more often than other years because the frequency of  
247 selection is proportionate to the weights. We first perform this bootstrapping process for  
248 the first dekad of MAM, comprised of 10 daily values of precipitation and temperature  
249 maximum and minimum. In order to build the scenarios for the first dekad of the MAM  
250 season for any target year, we sampled the first dekad of the MAM season from all years  
251 (1993-2012, except the target year) as described previously.
- 252 6. We then repeat this process for subsequent dekads of the MAM season. For example, Fig.  
253 4 shows the frequency of years in the available record (1993-2012) picked in generating  
254 100 climate scenarios for the MAM season of the year 2011, which was a drought year.  
255 Based on our estimates, year 2011 was most similar to the years 2009, 1999, and 2000,  
256 which were all drought years. Beyond the MAM season our bootstrapping selection is  
257 based on the equiprobable weights (similar to climatological forecasts).

258 For generating seasonal hydrologic forecasts (section 2.4) we only use 30 of those climate  
259 scenarios. Although all 30 scenarios aggregated over the MAM season are similar for any given

260 target year, the bootstrapping process described above allows for uncertainties in the evolution of  
261 daily weather pattern among each scenarios.

## 262 **2.4 Seasonal hydrologic forecasts**

263 Two sets of hindcast SM forecasts were generated by combining the antecedent  
264 conditions, one at March 5<sup>th</sup> and one April 5<sup>th</sup> (1993-2012), with a suite of climate scenarios  
265 (daily precipitation, maximum and minimum temperature, as described in section 2.3b) for the  
266 remainder of the season. (Note that the same climate scenarios were used in both cases). We  
267 chose these dates because March 5<sup>th</sup> is near the SOS and about a week before FEWS NET’s  
268 seasonal forecast review meeting in March; likewise, April 5<sup>th</sup> is near the middle-of-season  
269 (MOS) and about a week before the seasonal forecast review meeting in April.

270 For comparison, we also generated two more sets of forecasts using the Ensemble  
271 Streamflow Prediction (ESP) method (Shukla and Lettenmaier, 2011; Wood and Lettenmaier,  
272 2008; Wood et al., 2002). In this method, seasonal hydrologic forecasts are generated by driving  
273 the hydrologic model with atmospheric forcings sampled from the climatology. It is assumed that  
274 the climate during the upcoming season has equal likelihood of being similar to any of the years  
275 during the climatological period (1993-2012 in this case). The forecasts are initialized using  
276 “true” initial hydrologic conditions (IHCs), so the source of hydrologic forecast skill is only the  
277 IHCs. We used the SM forecast generated using the ESP method as a baseline to compare the  
278 similar forecasts generated using CFSv2 based seasonal climate scenarios (section 2.3). This  
279 comparison was done in order to examine the value of CFSv2 based climate scenarios in  
280 hydrologic forecasting, since both methods share the IHCs but differ in the climate scenarios.

### 281 **3. Evaluation of VIC derived soil moisture for agricultural drought** 282 **assessment**

283 First we evaluated the suitability of VIC-derived SM (generated by forcing the VIC  
284 model with high quality observed forcings (section 2.2)) for providing agricultural drought  
285 assessments across our domain (Fig. 1). Hereafter we refer to this dataset as “SM a posteriori  
286 estimates”. We did so by comparing SM a posteriori estimates, spatially aggregated over the  
287 crop zones only, with the Water Requirement Satisfaction Index (WRSI) (Verdin and Klaver,  
288 2002). WRSI is a water balance model that is used by Food and Agricultural Organization  
289 (FAO) as well as FEWS NET scientists to provide crop yield assessment (Senay and Verdin,  
290 2003; Verdin and Klaver, 2002; Verdin et al., 2005), therefore we used WRSI in lieu of actual  
291 crop yield data, which is generally scarce for this region. WRSI was calculated using the same  
292 precipitation data (i.e. CHIRPS) as VIC’s SM. WRSI is approximately equal to the percent of  
293 potential evapotranspiration met by available water resources, either rainfall or SM. As such,  
294 WRSI values range from 0 to 100, with a value below 50 commonly being associated with crop  
295 failure. Because only a limited amount of excess water is retained for the next time interval in  
296 the WRSI model, the relationship of seasonal precipitation with WRSI is not entirely linear. For  
297 example, WRSI values may be the same for 100% of normal precipitation and 120% of normal  
298 precipitation, since both precipitation values meet the required available moisture for crop  
299 growth. For this reason we compared standardized anomalies of SM, rainfall and WRSI over the  
300 crop zones. As shown in Fig. 6, the spearman rank correlation between rainfall and WRSI is 0.83  
301 and the correlation between SM and WRSI is slightly less (0.75). We chose the spearman rank  
302 correlation value to make sure that the correlation value is not sensitive to a few outlier years,  
303 given the small sample size. Based on this finding we postulate that VIC derived SM is a

304 reasonable indicator of agricultural drought in the focus domain.

305         Next we compared SM a posteriori estimates with the European Space Agency (ESA)  
306 Essential Climate Variable (ECV) SM dataset. This dataset is one of the most complete and long  
307 term global SM datasets based on active and passive microwave remote sensing. Further details  
308 about this dataset can be found in Liu et al. (2011) and (2012). For the comparison between both  
309 datasets we calculated standardized anomaly (anomaly divided by the standard deviation) using  
310 the climatology of 1993-2012. In Fig. 6 we present the comparison of both data sets for two  
311 above normal MAM SM years (1998 and 2010) and two below normal SM years (2000 and  
312 2011). Although the intensity of SM anomalies are different between both datasets (which partly  
313 could be attributed to VIC SM being from a much deeper soil profile than ECV SM dataset),  
314 overall both datasets do agree on the general direction of the anomaly, meaning that, according  
315 to both datasets, 1998 and 2010 were wet years and 2000 and 2011 were drought years. We  
316 observed similar agreement between both datasets in other years as well (not shown here).

#### 317 **4. Evaluation of precipitation and soil moisture forecasts**

318         Next we assessed the skill of the precipitation and SM forecasts. Our model hindcasts  
319 consisted of an ensemble of 30 precipitation and SM scenarios for each year in 1993-2012. We  
320 used the ensemble median of the scenarios and correlated this with the observed seasonal  
321 outcome. We used the CHIRPS to assess the skill of the precipitation forecasts and SM a  
322 posteriori estimates to assess the skill of the SM forecasts. We did so due to the lack of long-term  
323 SM observations for the region.

324         We compared the spatially aggregated (over the focus domain) MAM seasonal  
325 precipitation forecasts made during 1993-2012 and observations (CHIRPS) (Fig. 7). The value of



326 spearman rank correlation between precipitation forecasts and observations is 0.67.

327 Fig. 8 (a) shows the skill of SM forecasts initialized on March 5<sup>th</sup> (SOS) for lead-time of  
328 1 to 3 months. (Where lead-1 is the month of March and lead-3 is the month of May). The skill is  
329 defined as the spearman rank correlation between the ensemble median of all 30 SM scenarios  
330 for each year and SM a posteriori estimates (section 2.2). SM forecast skill is generally greater  
331 than 0.5 across the most of the region and greater than 0.9 for some parts at the 1-month lead.  
332 The SM forecast skill dissipates as the time between forecast month and day of forecast  
333 initialization increases. This finding about the SM forecast skill is consistent with the results of  
334 other studies (Mo et al., 2012; Shukla and Lettenmaier, 2011; Shukla et al., 2013). Nevertheless,  
335 over part of the focus domain (southeastern parts of Ethiopia, eastern parts of Kenya, as well as  
336 southern Somalia) the SM forecast skill remains as high as 0.5 for up to three months lead-time.  
337 This observation is particularly important in an early warning context, since it implies that over  
338 those regions skillful assumptions about the agricultural drought can be made early in the  
339 growing season. This lead-time is particularly helpful for FEWS NET food analysts, who can  
340 provide advanced warning about potential growing conditions in those regions.

341 Fig. 8(b) shows the SM forecast skill generated using the ESP method. As previously  
342 noted the ESP method does not derive its skill from the climate forecasts and is solely based on  
343 the knowledge of the IHCs (Shukla and Lettenmaier, 2011), therefore the comparison between  
344 Fig. 8 (a) and (b) shows the value of using skillful climate scenarios in improving SM forecast  
345 skill. This value is especially highlighted at lead-2 to 3 months (when the influence of the IHCs  
346 has diminished) when Fig. 8(a) shows higher level of skill than Fig. 8 (b).

347 We also calculated the SM forecast skill derived using CFSv2 based climate scenarios  
348 and the ESP method but during the forecast period starting on April 5<sup>th</sup> (Fig. 9 a and b,

349 respectively). Although SM forecast skill dissipates as one moves further from the initial state,  
350 one noteworthy observation from this figure is the higher SM forecast skill over the second and  
351 third month (lead-1 and lead-2 months respectively) of the MAM season. Comparing lead-2 and  
352 lead-3 forecasts skill in Fig. 8(a) with lead-1 and lead-2 forecast skill in Fig. 9(a), we see the  
353 higher values across the region in Fig. 9(a), corresponding to improved EOS information at the  
354 beginning of April compared to March. Ideally, forecasts of agricultural drought are early in the  
355 season; however, mid-season is the time when the antecedent SM state has a larger influence  
356 over SM until end-of-season. Such mid-season outlooks still lead actual harvest dates by several  
357 months, and can therefore provide critical early warning. This also highlights the value of  
358 incorporating precipitation during the early part of the season, which is reflected in the initial  
359 hydrologic state of the MOS. What this means, in practical terms, is that in case of delayed onset  
360 of rainfall and/or below normal rainfall during the first month of the season, SM at the middle of  
361 the season will be below normal and chances of recovery from the SM deficit (or failure of the  
362 crop) becomes lower (higher) than what they are at the beginning of the season. Again, a  
363 comparison of Fig. 9 (a) with Fig. 9(b) indicates that climate scenarios add to the SM forecast  
364 skill beyond the ESP method.

365         Although Figs. 8 and 9 show that SM forecasts generated using CFSv2 based climate  
366 scenarios are skillful, one obvious question is how this system would have performed during the  
367 2011 MAM season, which was one of the worst drought events in the history of this region. To  
368 answer this question, in Fig. 10 we compared the standardized anomaly of SM forecasts  
369 (generated by using CFSv2 based climate scenarios) initialized on March 5<sup>th</sup> (top panel) and  
370 April 5<sup>th</sup> (middle panel) with SM a posteriori estimates (bottom panel). From this figure (Fig. 10)  
371 it appears that although this system would have successfully predicted 2011 as a drought year as

372 early as March 5<sup>th</sup>, it would have underestimated the drought's severity. Forecasts made on April  
373 5<sup>th</sup> do show elevated drought severity, though, because they used updated (drier than normal)  
374 IHCs.

375 Finally we examine how the SM forecast skill varies among other drought years vs  
376 normal years by estimating the spatial pattern correlation between SM forecasts (generated using  
377 CFSv2 based seasonal climate scenarios) and SM a posteriori estimates over the region (Fig. 11).  
378 The higher the correlation, the better the forecast is in capturing the spatial variability of SM  
379 anomaly pattern. Spatial anomaly pattern correlation is greater than 0.60 for all years (Fig. 10).  
380 As indicated by Fig. 10, there is a correlation of -0.62 between spatial anomaly pattern  
381 correlation for MAM SM and standardized anomaly of MAM precipitation, which means that  
382 spatial anomaly pattern correlation is generally higher (lower) for negative (positive) anomaly of  
383 precipitation. In almost all years (except one) the value of spatial anomaly pattern correlation is  
384 greater than 0.8 when MAM precipitation anomaly was negative (i.e. meteorological drought  
385 years). This finding indicates that, in terms of capturing spatial variability of SM, this system  
386 does relatively better during drought years than in normal or above normal years.

## 387 **5. Concluding remarks**

388 Our primary findings are as follows:

- 389 1. VIC model derived SM values over the crop zones of the focus domain aligns well with  
390 end-of-season WRSI, the FAO indicator that is often used for providing crop yield  
391 assessments.
- 392 2. The hybrid approach that utilizes dynamical CFSv2 precipitation forecasts over EA and  
393 the Indo-Pacific Ocean to statistically forecast rainfall over the focus domain is more

394 skillful (correlation = 0.67 for MAM precipitation forecasts initialized in February) than  
395 using climatology (ESP) alone.

396 3. Forecasts initialized mid-season make the greatest contribution to end-of-season SM  
397 forecast skill. SM forecasts initialized at the beginning of the season were skillful across  
398 the domain at 1-month lead, while the forecast skill during the second and third months  
399 of the season increased when the SM forecast was initialized with updated initial  
400 hydrologic state, even with the same climate scenarios used at the time of the start of the  
401 season.

402 4. Spatial anomaly pattern correlation between SM forecast and SM a posteriori estimates  
403 are generally higher ( $>0.8$ ) for drought years, indicating the value of this system during  
404 drought events, which is the primary focus of FEWS NET.

405 We described the development and implementation of a seasonal hydrologic forecast  
406 system that is being used by FEWS NET scientists to provide seasonal assessment of agricultural  
407 production for food-insecure regions of EA. This is certainly not the first attempt to provide  
408 seasonal hydrologic forecasts for EA. Our approach is most similar to Yuan et al. (2013) and  
409 Sheffield et al. (2013)'s Africa Flood and Drought Monitor as mentioned in section 2.

410 Specifically, we used the same model parameters and temperature and wind forcings. The main  
411 differences between our system and theirs are the high resolution, station intensive, bias-  
412 corrected CHIRPS precipitation forcings and the hybrid statistical-dynamical approach used for  
413 generating seasonal climate scenarios.

414 Besides the Africa Flood and Drought Monitor, other approaches have been developed for  
415 drought monitoring and forecasting for Africa or EA. Rojas et al. (2011) described a drought  
416 monitoring approach that utilizes Vegetation Health Index (VHI) from the Advanced Very High

417 Resolution Radiometer (AVHRR) averaged over the crop season. Anderson et al. (2012)  
418 suggested an approach that takes advantage of the relative strength of three different methods for  
419 obtaining SM estimates. Mwangi et al. (2013) examined the skill of Standardized Precipitation  
420 Index (SPI) forecasts based on European Centre for Medium-Range Weather Forecasts  
421 (ECMWF) and found that for MAM season the skill was generally below 0.4 for forecasts issued  
422 in February. Meroni et al. (2014) described an approach to provide early warning of unfavorable  
423 crop and pasture conditions using a statistical analysis of Early Observation Data. While these  
424 approaches are valuable contributions, it is important for FEWS NET to have an in-house  
425 platform to help provide seasonal assessment of agricultural drought conditions and meet the  
426 decision making needs of the food analysts. This also allows us to test different approaches to  
427 generate climate scenarios and estimate initial hydrologic state (approaches that we plan to  
428 implement in this system are described in further details in next section).

## 429 **6. Future directions:**

430 As mentioned before, this seasonal agricultural drought forecast system is already being  
431 used to provide scientific assessment of seasonal agricultural outlook. However, we  
432 acknowledge that further improvements to this system will better meet the decision-making  
433 needs of the food analysts. Three primary avenues of improvements in this system are:

### 434 **1. Improvement in the estimation of initial hydrologic state**

435 Differences in the way that hydrologic models partition precipitation into evapotranspiration  
436 and runoff, and their different water holding capacity, lead to differences in SM sensitivity to  
437 precipitation variability. These differences may lead to discrepancies among the model based  
438 SM drought estimates (Crow et al., 2012; Wang et al., 2010). Therefore we are transferring  
439 this agricultural drought forecast system to NASA's FEWS NET Land Data Assimilation

440 System, an instance of NASA's Land Information System (LIS) (Kumar et al., 2006) that  
441 includes hydrologic and soil water balance models such as Noah (Ek et al., 2003; Schaake et  
442 al., 1996) and WRSI (Verdin and Klaver, 2002; Verdin et al., 2005) in addition to VIC and  
443 will include other land surface models such as the Catchment model (Koster et al., 2000) in  
444 the near future.

445 Besides using a multimodel framework for seasonal agricultural drought forecasting,  
446 another promising approach that we plan to test is data assimilation. Previous works have  
447 shown that data assimilation improves estimates of SM and snow state in large scale  
448 hydrologic model (Andreadis and Lettenmaier, 2006; Kumar et al., 2008) leading to a higher  
449 hydrologic forecast skill. Therefore we will test if assimilating satellite based SM estimates  
450 (for top soil layer) and/or total water storage (as estimated by NASA's Gravity Recovery and  
451 Climate Experiment) improves our SM forecasts skill.

## 452 **2. Improvement in climate scenario building process**

453 For the current version of the seasonal agricultural drought forecast system we only use  
454 dynamical seasonal climate forecasts from CFSv2. However, NCEP's National Multi-model  
455 Ensemble system (NMME, <http://www.cpc.ncep.noaa.gov/products/NMME/>) includes five  
456 other models aside from CFSv2. Recent studies have demonstrated the value of using  
457 multimodel ensembles of seasonal forecasts relative to using just one of the models  
458 (Hagedorn et al., 2005; Kirtman et al., 2013; Lavers et al., 2009; Yuan and Wood, 2013).  
459 Therefore we plan to use NMME model ensembles to generate climate scenarios.

460 We also aim to test other statistical forecasting methods to improve the skill of climate  
461 scenarios. One of those methods was recently suggested by Nicholson (2014), who found

462 that atmospheric variables, when used as predictors, can provide higher rainfall forecast skill  
463 in the Greater Horn of Africa than other surface variables such as sea surface temperature  
464 (SST) and sea level pressure (SLP).

### 465 **3. Improvement in presentation of the forecasts**

466 The primary goal of this seasonal agricultural drought forecast system is to assist FEWS  
467 NET's food analysts with their decision making process. Hence it is imperative for us to  
468 provide forecasts in a manner that is easily understandable by the decision makers and still  
469 includes key information about the forecast (such as probabilities of a region being either wet  
470 or dry in an upcoming season). We recognize that this is a slow and iterative process;  
471 however, through this unique position of working directly with the food analysts we have the  
472 perfect opportunity to translate science into action. We plan to improve the presentation of  
473 our forecasts by incorporating the feedback of the end users (FEWS NET's food analysts)  
474 into our forecasts. Thus far we have learned that providing the forecasts in terms of the  
475 chances of drought onset/persistence/recovery and best analogs is well received.

### 476 **Acknowledgements**

477 This research was supported by the Postdocs Applying Climate Expertise (PACE) Fellowship  
478 Program, partially funded by the NOAA Climate Program Office and administered by the UCAR  
479 Visiting Scientist Programs. Additional support for this work was provided by the USAID's  
480 FEWS NET (USGS award #G09AC00001), NOAA Technical Transitions grant  
481 NA11OAR4310151 and NASA SERVIR grant XXXX. The authors would like to thank Diego  
482 Pedreros (USGS/UCSB) for his work on generating WRSI data.

483           Finally we also like to extend our thanks to Dr. Justin Sheffield, Nate Chaney, and others  
484 at Terrestrial Hydrology Research Group in the Department of Civil and Environmental  
485 Engineering at Princeton University for their work on developing forcing and model parameter  
486 datasets and kindly sharing them with us.

487

488



## 489 Reference

- 490 Adam, J. C., Haddeland, I., Su, F. and Lettenmaier, D. P.: Simulation of reservoir influences on annual and  
491 seasonal streamflow changes for the Lena, Yenisei, and Ob' rivers, *J. Geophys. Res.*, 112(D24),  
492 doi:10.1029/2007JD008525, 2007.
- 493 Anderson, W. B., Zaitchik, B. F., Hain, C. R., Anderson, M. C., Yilmaz, M. T., Mecikalski, J. and Schultz, L.:  
494 Towards an integrated soil moisture drought monitor for East Africa, *Hydrology and Earth System*  
495 *Sciences Discussions*, 9(4), 4587–4631, 2012.
- 496 Andreadis, K. M. and Lettenmaier, D. P.: Assimilating remotely sensed snow observations into a  
497 macroscale hydrology model, *Advances in Water Resources*, 29(6), 872–886, 2006.
- 498 Batjes, N. H.: A world dataset of derived soil properties by FAO–UNESCO soil unit for global modelling,  
499 *Soil use and management*, 13(1), 9–16, 1997.
- 500 Chaney, N., Sheffield, J., Villarini, G. and Wood, E. F.: Spatial analysis of trends in climatic extremes with  
501 a high resolution gridded daily meteorological data set over Sub-Saharan Africa, *J. Clim.*, doi:(in review),  
502 2013.
- 503 Checchi, F. and Robinson, W. C.: Mortality among populations of southern and central Somalia affected  
504 by severe food insecurity and famine during 2010–2012, FAO/FSNAU and FEWSNET. [online] Available  
505 from: [http://www.fsnau.org/in-focus/study-report-mortality-among-populations-southern-and-central-](http://www.fsnau.org/in-focus/study-report-mortality-among-populations-southern-and-central-somalia-affected-severe-food-)  
506 [somalia-affected-severe-food-](http://www.fsnau.org/in-focus/study-report-mortality-among-populations-southern-and-central-somalia-affected-severe-food-), 2013.
- 507 Cosby, B. J., Hornberger, G. M., Clapp, R. B. and Ginn, T. R.: A statistical exploration of the relationships  
508 of soil moisture characteristics to the physical properties of soils, *Water Resources Research*, 20(6), 682–  
509 690, 1984.
- 510 Crow, W. T., Kumar, S. V. and Bolten, J. D.: On the utility of land surface models for agricultural drought  
511 monitoring, *Hydrol. Earth Syst. Sci.*, 16(9), 3451–3460, doi:10.5194/hess-16-3451-2012, 2012.
- 512 Ek, M. B., Mitchell, K. E., Lin, Y., Rogers, E., Grunmann, P., Koren, V., Gayno, G. and Tarpley, J. D.:  
513 Implementation of Noah land surface model advances in the National Centers for Environmental  
514 Prediction operational mesoscale Eta model, *Journal of Geophysical Research: Atmospheres*, 108(D22),  
515 n/a–n/a, doi:10.1029/2002JD003296, 2003.
- 516 Funk, C., Dettinger, M. D., Michaelsen, J. C., Verdin, J. P., Brown, M. E., Barlow, M. and Hoell, A.:  
517 Warming of the Indian Ocean threatens eastern and southern African food security but could be  
518 mitigated by agricultural development, *Proc. Natl. Acad. Sci. U.S.A.*, 105(32), 11081–11086,  
519 doi:10.1073/pnas.0708196105, 2008.
- 520 Funk, C., Eilerts, G., Davenport, F. and Michaelsen, J.: A Climate Trend Analysis of Kenya—August 2010,  
521 USGS fact sheet, 2010.
- 522 Funk, C., Husak, G., Michaelsen, J., Shukla, S., Hoell, A., Lyon, B., Hoerling, M. P.,  
523 Liebmann, B., Zhang, T., Verdin, J., Galu, G., Eilerts, G., and Rowland, J.: Attribution of  
524 2012 and 2003–12 rainfall deficits in eastern Kenya and southern Somalia, *Bull. Amer.*

525 Meteor. Soc., 95, 2013.  
526

527 Funk, C., Hoell, A., Shukla, S., Bladé, I., Liebmann, B., Roberts, J. B., Robertson, F. R. and Husak, G.:  
528 Predicting East African spring droughts using Pacific and Indian Ocean sea surface temperature indices,  
529 Hydrol. Earth Syst. Sci. Discuss., 11(3), 3111–3136, doi:10.5194/hessd-11-3111-2014, 2014a.

530 Funk, C., Peterson, P., Landsfield, M., Pedreros, D., Verdin, J., Rowland, J., Romero, B., Husak, G.,  
531 Michaelson, J. and Vedin, A.: A Quasi-global Precipitation Time Series for Drought Monitoring, USGS,  
532 EROS Data Center. [online] Available from: <http://chg.geog.ucsb.edu/data/chirps.pdf>, 2014b.

533 Funk, C., Senay, G., Asfaw, A., Verdin, J., Rowland, J., Michaelson, J., Eilerts, G., Korecha, D. and  
534 Choularton, R.: Recent drought tendencies in Ethiopia and equatorial-subtropical eastern Africa, Famine  
535 Early Warning System Network, USAID, Washington, DC, 2005.

536 Hagedorn, R., Doblas-Reyes, F. J. and Palmer, T. N.: The rationale behind the success of multi-model  
537 ensembles in seasonal forecasting – I. Basic concept, Tellus A, 57(3), 219–233, doi:10.1111/j.1600-  
538 0870.2005.00103.x, 2005.

539 Hamill, T. M., Bates, G. T., Whitaker, J. S., Murray, D. R., Fiorino, M., Galarneau, T. J., Zhu, Y. and  
540 Lapenta, W.: NOAA’s Second-Generation Global Medium-Range Ensemble Reforecast Dataset, Bulletin  
541 of the American Meteorological Society, 94(10), 1553–1565, doi:10.1175/BAMS-D-12-00014.1, 2013.

542 Hidalgo, H. G., Dettinger, M. D. and Cayan, D. R.: Downscaling with constructed analogues: Daily  
543 precipitation and temperature fields over the United States, California Energy Commission PIER Final  
544 Project Report CEC-500-2007-123, 2008.

545 Hillier, D.: A dangerous delay: the cost of late response to early warnings in the 2011 drought in the  
546 Horn of Africa, Oxfam. [online] Available from:  
547 <http://books.google.com/books?hl=en&lr=&id=3c5o5gnSj74C&oi=fnd&pg=PA3&dq=Drought%2BFamine%2BEast+Africa&ots=Fdonfsy2jh&sig=pHT4RdBcOyDIbikstX0Xl7sb0sQ> (Accessed 26 June 2013), 2012.

549 Hoell, A. and Funk, C.: Indo-Pacific sea surface temperature influences on failed consecutive rainy  
550 seasons over eastern Africa, Clim Dyn, 1–16, doi:10.1007/s00382-013-1991-6, 2013a.

551 Hoell, A. and Funk, C.: The ENSO-related West Pacific Sea Surface Temperature Gradient, Journal of  
552 Climate, 130729124132007, doi:10.1175/JCLI-D-12-00344.1, 2013b.

553 Keyantash, J. and Dracup, J. A.: The quantification of drought: An evaluation of drought indices., Bulletin  
554 of the American Meteorological Society, 83, 1167–1180, 2002.

555 Kirtman, B. P., Min, D., Infanti, J. M., Kinter III, J. L., Paolino, D. A., Zhang, Q., van den Dool, H., Saha, S.,  
556 Mendez, M. P. and Becker, E.: The North American Multi-Model Ensemble (NMME): Phase-1 Seasonal to  
557 Interannual Prediction, Phase-2 Toward Developing Intra-Seasonal Prediction, Bulletin of the American  
558 Meteorological Society [online] Available from: <http://journals.ametsoc.org/doi/abs/10.1175/BAMS-D-12-00050.1> (Accessed 28 August 2013), 2013.

560 Koster, R. D., Mahanama, S. P. ., Livneh, B., Lettenmaier, D. P. and Reichle, R. H.: Skill in streamflow  
561 forecasts derived from large-scale estimates of soil moisture and snow, *Nature Geoscience*, 3(9), 613–  
562 616, 2010.

563 Koster, R. D., Suarez, M. J., Ducharne, A., Stieglitz, M. and Kumar, P.: A catchment-based approach to  
564 modeling land surface processes in a general circulation model: 1. Model structure, *Journal of*  
565 *Geophysical Research: Atmospheres*, 105(D20), 24809–24822, doi:10.1029/2000JD900327, 2000.

566 Kumar, S., Peterslidard, C., Tian, Y., Houser, P., Geiger, J., Olden, S., Lighty, L., Eastman, J., Doty, B. and  
567 Dirmeyer, P.: Land information system: An interoperable framework for high resolution land surface  
568 modeling, *Environmental Modelling & Software*, 21(10), 1402–1415, doi:10.1016/j.envsoft.2005.07.004,  
569 2006.

570 Kumar, S. V., Reichle, R. H., Peters-Lidard, C. D., Koster, R. D., Zhan, X., Crow, W. T., Eylander, J. B. and  
571 Houser, P. R.: A land surface data assimilation framework using the land information system: Description  
572 and applications, *Advances in Water Resources*, 31(11), 1419–1432,  
573 doi:10.1016/j.advwatres.2008.01.013, 2008.

574 Lavers, D., Luo, L. and Wood, E. F.: A multiple model assessment of seasonal climate forecast skill for  
575 applications, *Geophysical Research Letters*, 36, 209, 2009.

576 Liang, X., Lettenmaier, D. P., Wood, E. F. and Burges, S. J.: A simple hydrologically based model of land  
577 surface water and energy fluxes for general circulation models, *Journal of Geophysical Research:*  
578 *Atmospheres* (1984–2012), 99(D7), 14415–14428, 1994.

579 Liang, X., Wood, E. F. and Lettenmaier, D. P.: Surface soil moisture parameterization of the VIC-2L  
580 model: Evaluation and modification, *Global and Planetary Change*, 13(1), 195–206, 1996a.

581 Liang, X., Wood, E. F. and Lettenmaier, D. P.: Surface soil moisture parameterization of the VIC-2L  
582 model: Evaluation and modification, *Global and Planetary Change*, 13(1-4), 195–206, 1996b.

583 Liu, Y. Y., Dorigo, W. A., Parinussa, R. M., de Jeu, R. A. M., Wagner, W., McCabe, M. F., Evans, J. P. and  
584 van Dijk, A. I. J. M.: Trend-preserving blending of passive and active microwave soil moisture retrievals,  
585 *Remote Sensing of Environment*, 123, 280–297, doi:10.1016/j.rse.2012.03.014, 2012.

586 Liu, Y. Y., Parinussa, R. M., Dorigo, W. A., De Jeu, R. A. M., Wagner, W., van Dijk, A. I. J. M., McCabe, M. F.  
587 and Evans, J. P.: Developing an improved soil moisture dataset by blending passive and active  
588 microwave satellite-based retrievals, *Hydrol. Earth Syst. Sci.*, 15(2), 425–436, doi:10.5194/hess-15-425-  
589 2011, 2011.

590 Livneh, B., Rosenberg, E. A., Lin, C., Nijssen, B., Mishra, V., Andreadis, K. M., Maurer, E. P. and  
591 Lettenmaier, D. P.: A Long-Term Hydrologically Based Dataset of Land Surface Fluxes and States for the  
592 Conterminous United States: Update and Extensions\*, *Journal of Climate*, 26(23), 9384–9392,  
593 doi:10.1175/JCLI-D-12-00508.1, 2013.

594 Lyon, B. and DeWitt, D. G.: A recent and abrupt decline in the East African long rains, *Geophysical*  
595 *Research Letters*, 39(2), n/a–n/a, doi:10.1029/2011GL050337, 2012.

596 Maurer, E. P., Wood, A. W., Adam, J. C., Lettenmaier, D. P. and Nijssen, B.: A Long-Term Hydrologically  
597 Based Dataset of Land Surface Fluxes and States for the Conterminous United States\*, *Journal of*  
598 *Climate*, 15(22), 3237–3251, 2002.

599 Meroni, M., Fasbender, D., Kayitakire, F., Pini, G., Rembold, F., Urbano, F. and Verstraete, M. M.: Early  
600 detection of biomass production deficit hot-spots in semi-arid environment using FAPAR time series and  
601 a probabilistic approach, *Remote Sensing of Environment*, 142, 57–68, doi:10.1016/j.rse.2013.11.012,  
602 2014.

603 Mo, K. C., Shukla, S., Lettenmaier, D. P. and Chen, L.-C.: Do Climate Forecast System (CFSv2) forecasts  
604 improve seasonal soil moisture prediction?, *Geophysical Research Letters*, 39(23), n/a–n/a,  
605 doi:10.1029/2012GL053598, 2012.

606 Mosley, J.: Translating Famine Early Warning into Early Action: An East Africa Case Study, [online]  
607 Available from:  
608 [http://www.chathamhouse.org/sites/default/files/public/Research/Africa/1112pp\\_mosley.pdf](http://www.chathamhouse.org/sites/default/files/public/Research/Africa/1112pp_mosley.pdf)  
609 (Accessed 26 June 2013), 2012.

610 Mwangi, E., Wetterhall, F., Dutra, E., Giuseppe, F. D. and Pappenberger, F.: Forecasting droughts in East  
611 Africa, *Hydrology and Earth System Sciences Discussions*, 10(8), 10209–10230, 2013.

612 Myneni, R. B., Ramakrishna, R., Nemani, R. and Running, S. W.: Estimation of global leaf area index and  
613 absorbed PAR using radiative transfer models, *Geoscience and Remote Sensing, IEEE Transactions on*,  
614 35(6), 1380–1393, 1997.

615 Nicholson, S. E.: The predictability of rainfall over the Greater Horn of Africa. Part I. Prediction of  
616 seasonal rainfall., *Journal of Hydrometeorology*, 140117143344004, doi:10.1175/JHM-D-13-062.1, 2014.

617 Nijssen, B., Lettenmaier, D. P., Liang, X., Wetzel, S. W. and Wood, E. F.: Streamflow simulation for  
618 continental-scale river basins, *Water Resources Research*, 33(4), 711–724, 1997.

619 Nijssen, B., O'Donnell, G. M., Hamlet, A. F. and Lettenmaier, D. P.: Hydrologic sensitivity of global rivers  
620 to climate change, *Climatic Change*, 50(1), 143–175, 2001a.

621 Nijssen, B., O'Donnell, G. M., Lettenmaier, D. P., Lohmann, D. and Wood, E. F.: Predicting the Discharge  
622 of Global Rivers, *Journal of Climate*, 14(15), 3307–3323, doi:10.1175/1520-  
623 0442(2001)014<3307:PTDOGR>2.0.CO;2, 2001b.

624 Owiti, Z., Ogallo, L. A. and Mutemi, J.: Linkages between the Indian Ocean Dipole and east African  
625 seasonal rainfall anomalies, *Journal of Kenya Meteorological Society Volume*, 2, 1, 2008.

626 Pricope, N. G., Husak, G., Lopez-Carr, D., Funk, C. and Michaelsen, J.: The climate-population nexus in  
627 the East African Horn: Emerging degradation trends in rangeland and pastoral livelihood zones, *Global*  
628 *Environmental Change*, 23(6), 1525–1541, doi:10.1016/j.gloenvcha.2013.10.002, 2013.

629 Rojas, O., Vrieling, A. and Rembold, F.: Assessing drought probability for agricultural areas in Africa with  
630 coarse resolution remote sensing imagery, *Remote Sensing of Environment*, 115(2), 343–352,  
631 doi:10.1016/j.rse.2010.09.006, 2011.

632 Schaake, J. C., Koren, V. I., Duan, Q.-Y., Mitchell, K. and Chen, F.: Simple water balance model for  
633 estimating runoff at different spatial and temporal scales, *Journal of Geophysical Research:*  
634 *Atmospheres*, 101(D3), 7461–7475, doi:10.1029/95JD02892, 1996.

635 Senay, G. B. and Verdin, J.: Characterization of yield reduction in Ethiopia using a GIS-based crop water  
636 balance model, *Canadian Journal of Remote Sensing*, 29(6), 687–692, 2003.

637 Sheffield, J., Goteti, G. and Wood, E. F.: Development of a 50-year high-resolution global dataset of  
638 meteorological forcings for land surface modeling, *Journal of Climate*, 19(13), 3088–3111,  
639 doi:10.1175/JCLI3790.1, 2006.

640 Sheffield, J., Wood, E. F., Chaney, N., Guan, K., Sadri, S., Yuan, X., Olang, L., Amni, A., Ali, A. and Demuth,  
641 S.: A Drought Monitoring and Forecasting System for Sub-Sahara African Water Resources and Food  
642 Security, *Bull. Am. Met. Soc.*, doi:(in review), 2013.

643 Shukla, S. and Lettenmaier, D. P.: Seasonal hydrologic prediction in the United States: understanding the  
644 role of initial hydrologic conditions and seasonal climate forecast skill, *Hydrol. Earth Syst. Sci.*, 15(11),  
645 3529–3538, doi:10.5194/hess-15-3529-2011, 2011.

646 Shukla, S., Sheffield, J., Wood, E. F. and Lettenmaier, D. P.: On the sources of global land surface  
647 hydrologic predictability, *Hydrol. Earth Syst. Sci.*, 17(7), 2781–2796, doi:10.5194/hess-17-2781-2013,  
648 2013.

649 Tierney, J. E., Smerdon, J. E., Anchukaitis, K. J. and Seager, R.: Multidecadal variability in East African  
650 hydroclimate controlled by the Indian Ocean, *Nature*, 493(7432), 389–392, doi:10.1038/nature11785,  
651 2013.

652 Todini, E.: The ARNO rainfall–runoff model, *Journal of Hydrology*, 175(1-4), 339–382, 1996.

653 Troy, T. J., Wood, E. F. and Sheffield, J.: An efficient calibration method for continental-scale land surface  
654 modeling, *Water Resources Research*, 44(9) [online] Available from:  
655 <http://www.agu.org/journals/wr/wr0809/2007WR006513/2007wr006513-t02.txt> (Accessed 17  
656 September 2013), 2008.

657 Verdin, J., Funk, C., Senay, G. and Choularton, R.: Climate science and famine early warning,  
658 *Philosophical Transactions of the Royal Society B: Biological Sciences*, 360(1463), 2155–2168, 2005.

659 Verdin, J. and Klaver, R.: Grid-cell-based crop water accounting for the famine early warning system,  
660 *Hydrological Processes*, 16(8), 1617–1630, 2002.

661 Wang, A., Bohn, T. J., Mahanama, S. P., Koster, R. D. and Lettenmaier, D. P.: Multimodel ensemble  
662 reconstruction of drought over the continental United States,, 2010.

663 Williams, A. P. and Funk, C.: A westward extension of the warm pool leads to a westward extension of  
664 the Walker circulation, drying eastern Africa, *Climate Dynamics*, 37(11-12), 2417–2435,  
665 doi:10.1007/s00382-010-0984-y, 2011.

666 Wood, A. W. and Lettenmaier, D. P.: An ensemble approach for attribution of hydrologic prediction  
667 uncertainty, *Geophysical Research Letters*, 35(14), L14401, 2008.

668 Wood, A. W., Maurer, E. P., Kumar, A. and Lettenmaier, D. P.: Long-range experimental hydrologic  
669 forecasting for the eastern United States, *J. Geophys. Res.*, 107(D20), 4429, doi:10.1029/2001JD000659,  
670 2002.

671 Yuan, X. and Wood, E. F.: Multimodel seasonal forecasting of global drought onset, *Geophys. Res. Lett.*,  
672 40(18), 4900–4905, doi:10.1002/grl.50949, 2013.

673 Yuan, X., Wood, E. F., Chaney, N. W., Sheffield, J., Kam, J., Liang, M. and Guan, K.: Probabilistic Seasonal  
674 Forecasting of African Drought by Dynamical Models, *Journal of Hydrometeorology*, 14(6), 1706–1720,  
675 doi:10.1175/JHM-D-13-054.1, 2013a.

676 Yuan, X., Wood, E. F., Roundy, J. K. and Pan, M.: CFSv2-Based Seasonal Hydroclimatic Forecasts over the  
677 Conterminous United States, *J. Climate*, 26(13), 4828–4847, doi:10.1175/JCLI-D-12-00683.1, 2013b.

678

679

680

681 **List of figures:**

682 Figure 1: Ratio of March-April-May (MAM) precipitation with the annual precipitation  
683 (calculated using Climate Hazards Group InfraRed Precipitation with Station data (CHIRPS))  
684 over the focus domain that expands over parts of Ethiopia, Kenya and Somalia. This region was  
685 the epicenter of the 2011 humanitarian disaster.

686 Figure 2: Schematic diagram summarizing the approach, data, and models used for the  
687 development and implementation of current version of Seasonal Agricultural Drought Forecast  
688 system.

689 Figure 3: Spatial pattern of correlation between CFSv2 precipitation forecasts for MAM season  
690 (initialized in February) and observed MAM rainfall (CHIRPS) in the focus domain. Correlation  
691 values have been masked for significance (values  $r < |0.35|$  have been screened).

692 Figure 4: Frequency of picking each climatological year for generating 30 climate scenarios for  
693 MAM season of the year 2011. Top panel shows the frequency that resulted from conditioning  
694 bootstrapping process to CFSv2-based weighted probabilities and the bottom panel shows the  
695 same but for climatological forecasts where each year was assigned the same probability.

696 Figure 5: Comparison of MAM precipitation, SM a posteriori estimates (VIC-SM) and end-of-  
697 season Water Requirement Satisfaction Index (WRSI) for crop zones in the focus domain for  
698 each year between 1993-2012.

699 Figure 6: Comparison standardized anomaly SM a posteriori estimates (VIC-SM, sum of  
700 moisture in top two layers) and ECV microwave soil moisture (MW-SM) for March through  
701 May season of the years (a) 1998 (b) 2000 (c) 2009 and (d) 2010.

702 Figure 7: Comparison of ensemble median MAM precipitation forecasts and observations  
703 (CHIPRS) spatially aggregated over the focus domain.

704 Figure 8: Skill of soil moisture forecasts (i.e. correlation between ensemble median of soil  
705 moisture forecasts and a posteriori estimates) initialized on March 4<sup>th</sup> (start of the season)  
706 estimated using (a) CFSv2 based seasonal climate scenarios, (b) ESP method.

707 Figure 9: Same as in Fig. 8 but for forecasts initialized on April 5<sup>th</sup> (middle-of-season)

708 Figure 10: Comparison of standardized anomaly of SM forecast generated using CFSv2 based  
709 seasonal climate scenarios with SM a posteriori estimates during MAM season of the year 2011.  
710 Top panel shows March through May forecasts generated on March 5<sup>th</sup>, middle panel shows the  
711 same for April and May generated on April 5<sup>th</sup> and bottom panel shows the SM a posteriori  
712 estimates.

713 Figure 11: Comparison between spatial anomaly pattern correlation (between MAM mean soil  
714 moisture forecast initialized at the start of season and observation) and standardized anomaly of  
715 MAM precipitation. This plot indicates that spatial anomaly pattern correlation is generally  
716 higher ( $> 0.8$ ) during drought years (when standardized anomaly of MAM precipitation is  $< 0$ ).

717

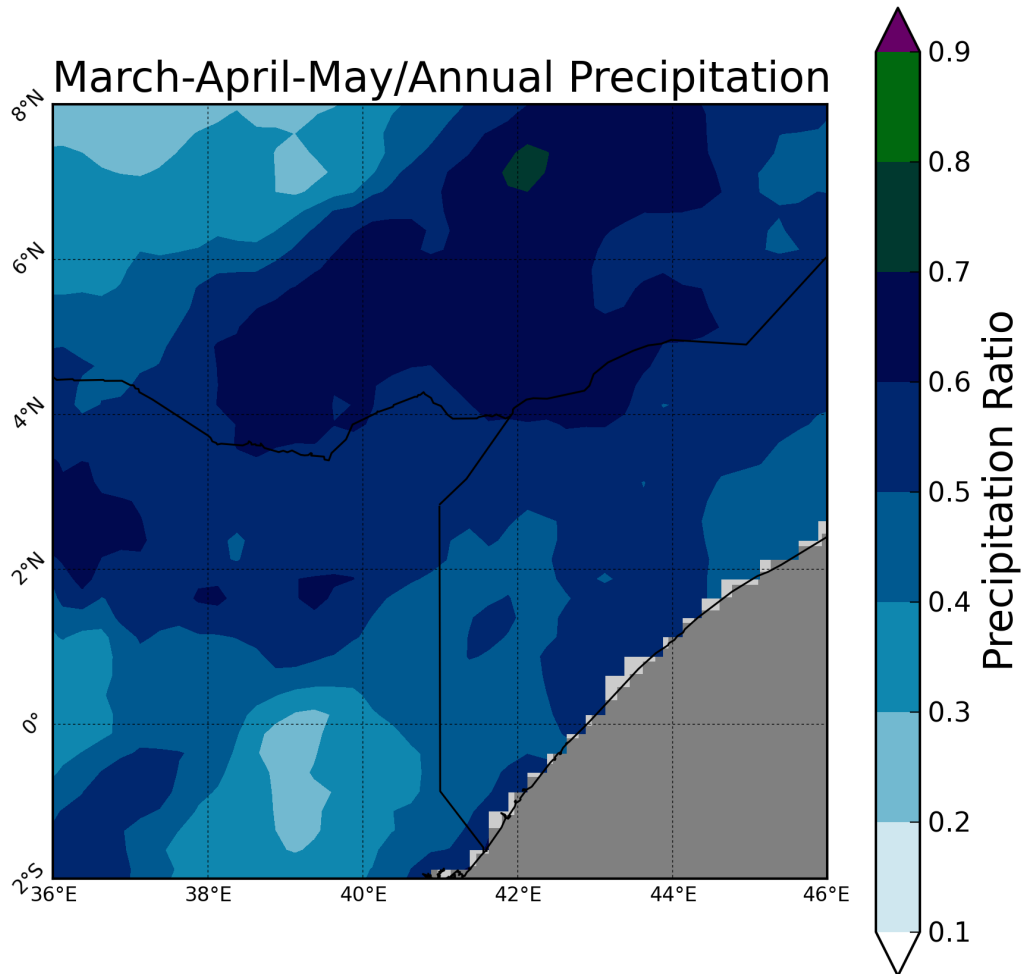
718

719



720

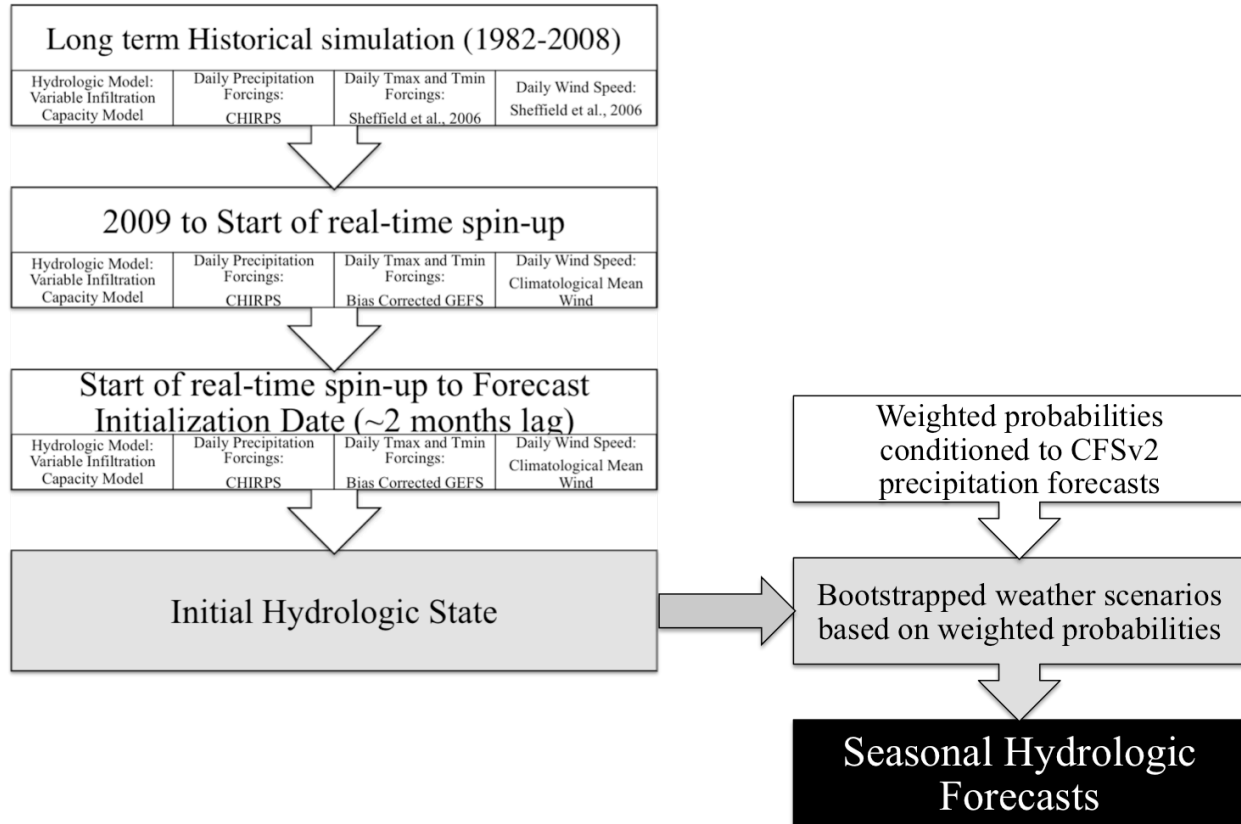
721



722

723 Figure 1: Ratio of March-April-May (MAM) precipitation with the annual precipitation  
724 (calculated using Climate Hazards Group InfraRed Precipitation with Station data (CHIRPS))  
725 over the focus domain that expands over parts of Ethiopia, Kenya and Somalia. This region was  
726 the epicenter of the 2011 humanitarian disaster.

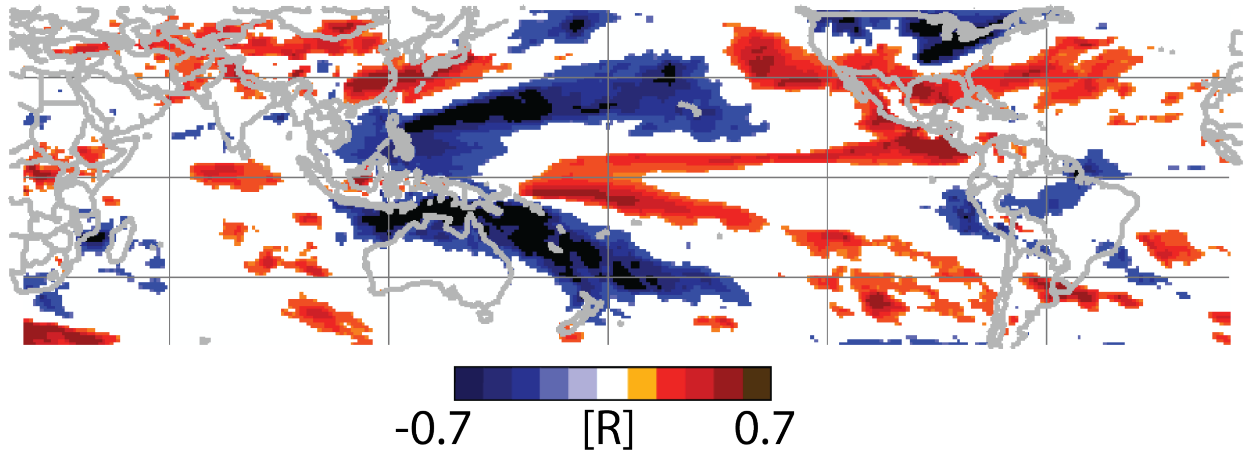
727



728

729 Figure 2: Schematic diagram summarizing the approach, data, and models used for the  
 730 development and implementation of current version of Seasonal Agricultural Drought Forecast  
 731 system.

732



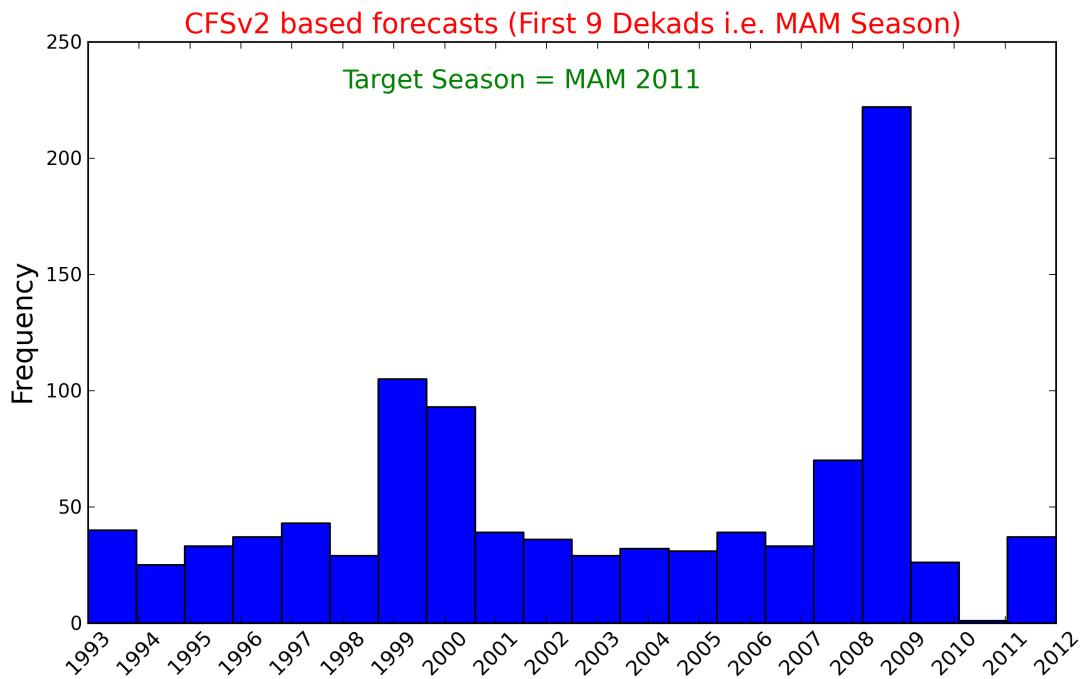
733

734 Figure 3: Spatial pattern of correlation between CFSv2 precipitation forecasts for MAM season  
735 (initialized in February) and observed MAM rainfall (CHIRPS) in the focus domain. Correlation  
736 values have been masked for significance (values  $r < |0.35|$  have been screened).

737

738

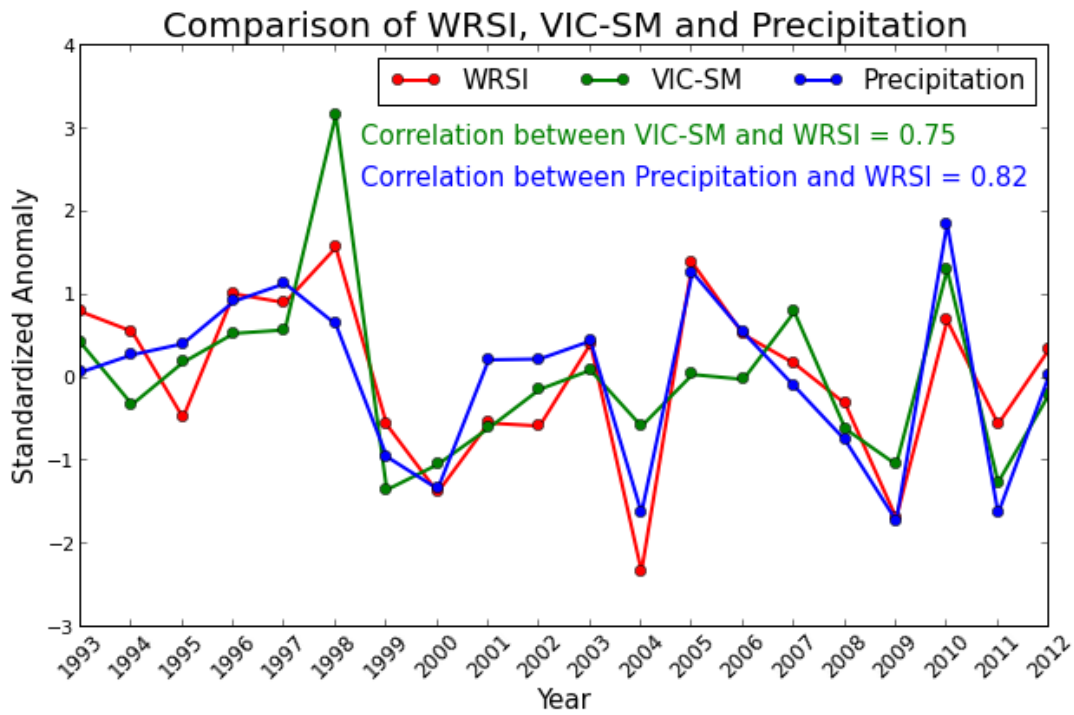
739



740

741 Figure 4: Frequency of picking each climatological year for generating 30 climate scenarios for  
 742 MAM season of the year 2011. Top panel shows the frequency that resulted from conditioning  
 743 bootstrapping process to CFSv2 based weighted probabilities and the bottom panel shows the  
 744 same but for climatological forecasts where each year was assigned the same probability.

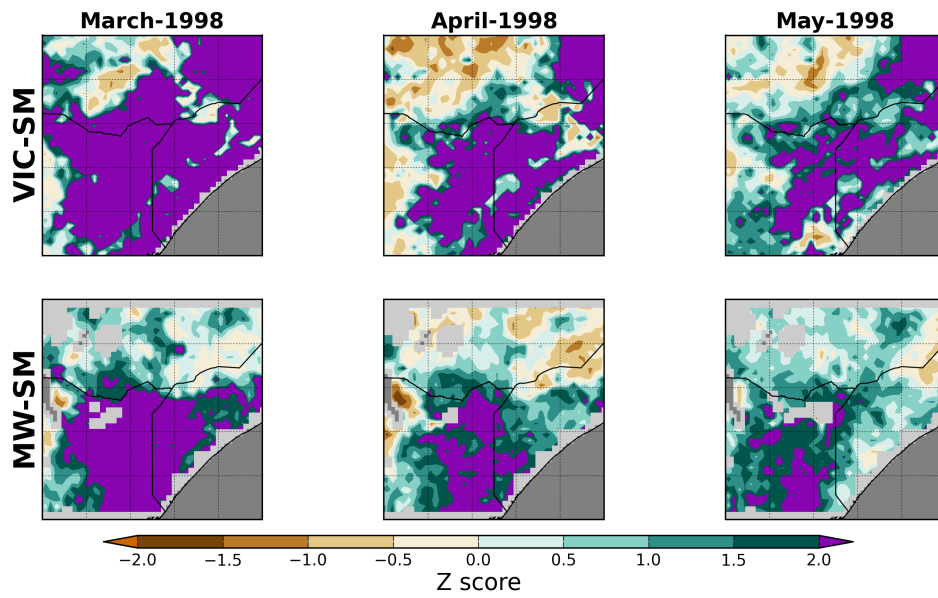
745



746

747 Figure 5: Comparison of MAM precipitation, SM a posteriori estimates (VIC-SM) and end-of-  
 748 season Water Requirement Satisfaction Index (WRSI) for crop zones in the focus domain for  
 749 each year between 1993-2012.

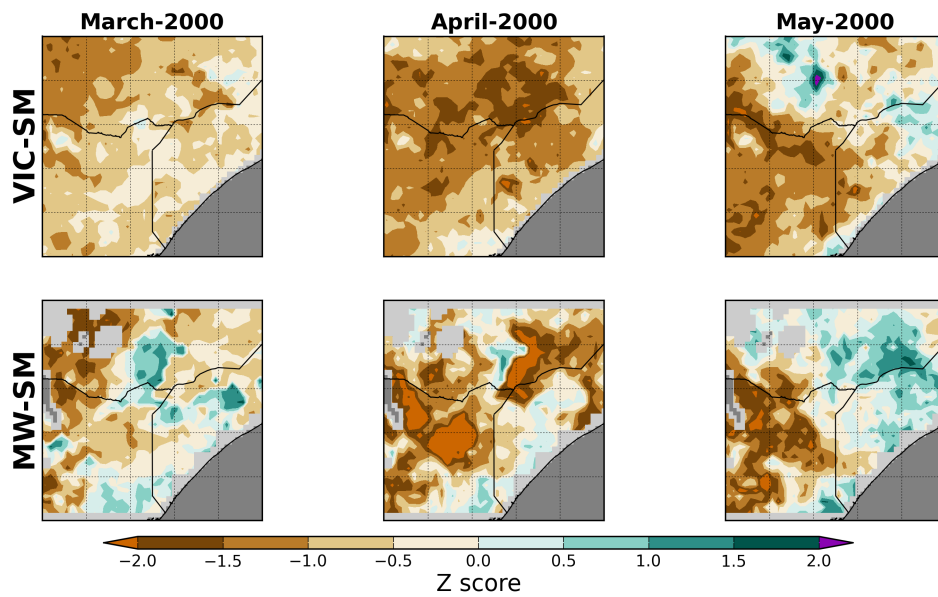
750



751

752

(a)

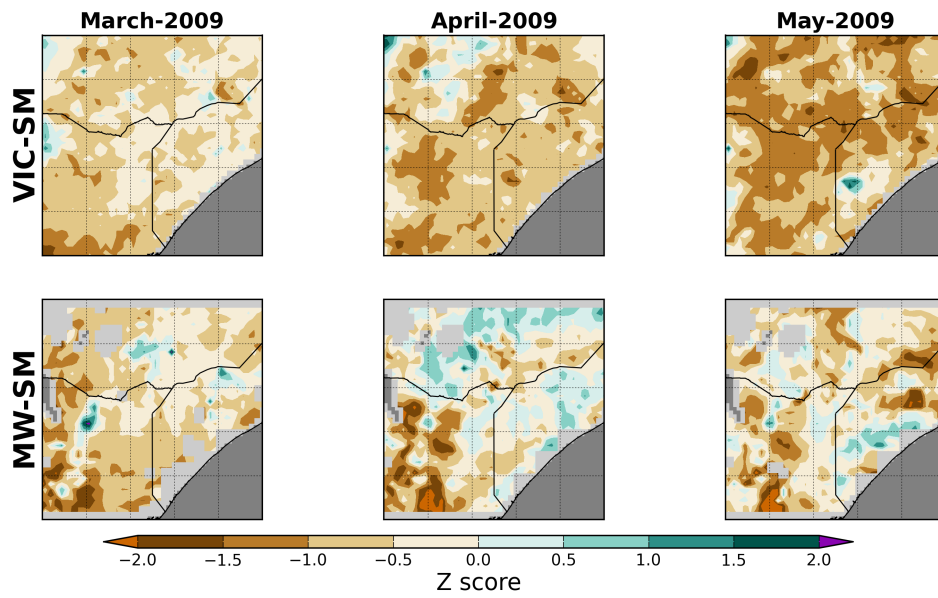


753

754

755

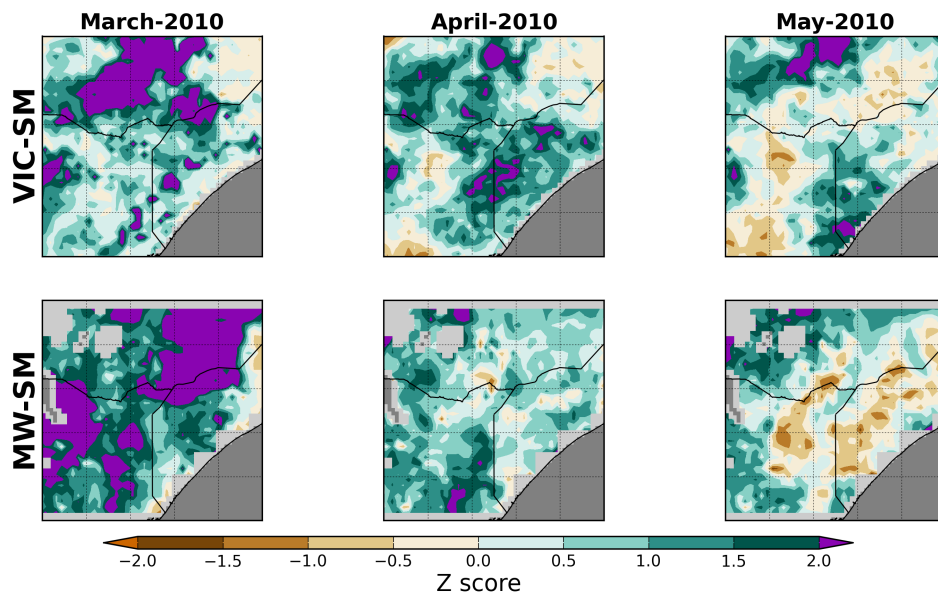
(b)



756

757

(c)



758

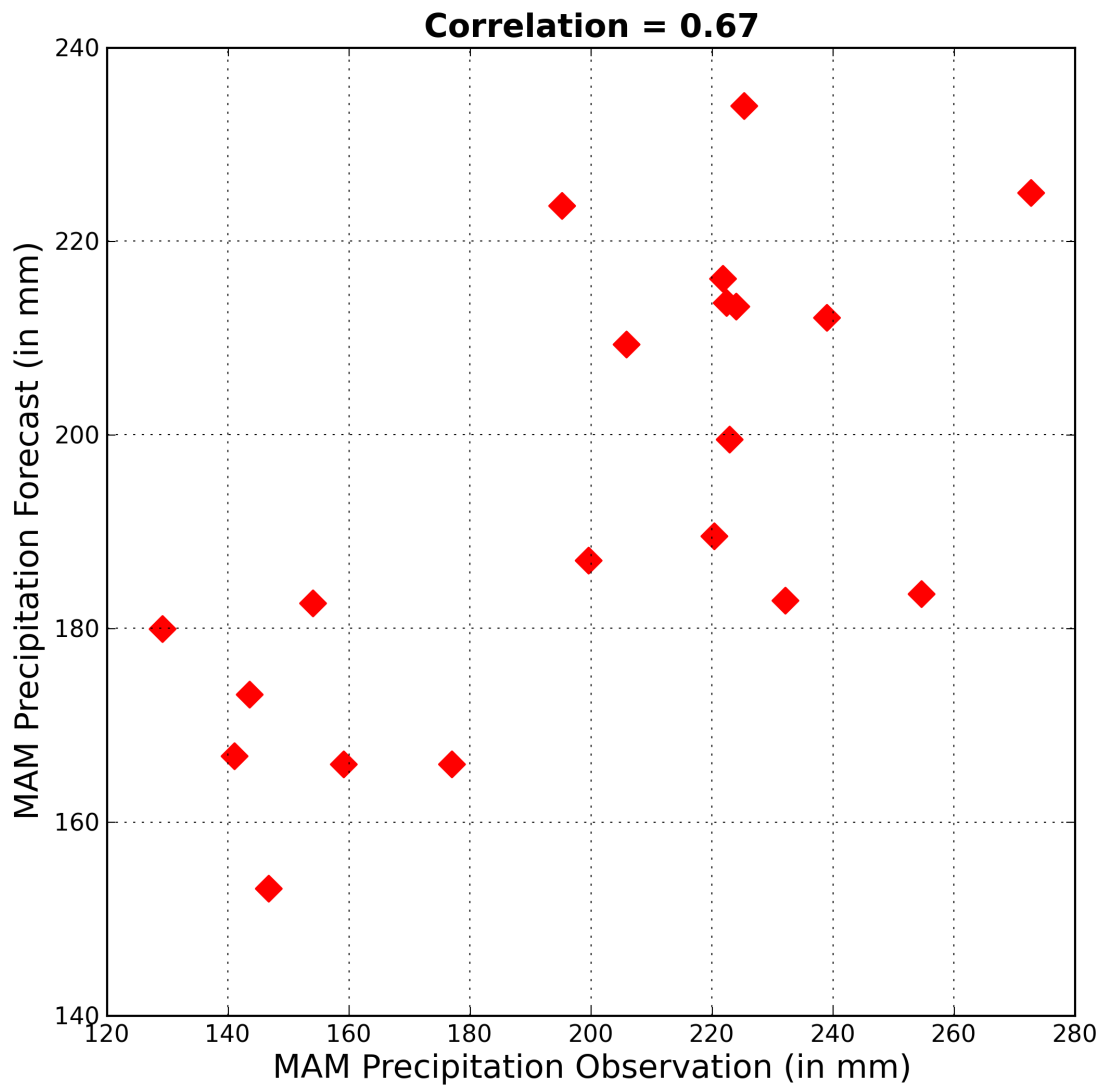
759

(d)

760 Figure 6: Comparison standardized anomaly SM a posteriori estimates (VIC-SM, sum of  
 761 moisture in top two layers), and ECV microwave soil moisture (MW-SM) for the March through  
 762 May season of the years (a) 1998 (b) 2000 (c) 2009 and (d) 2010.

763

764



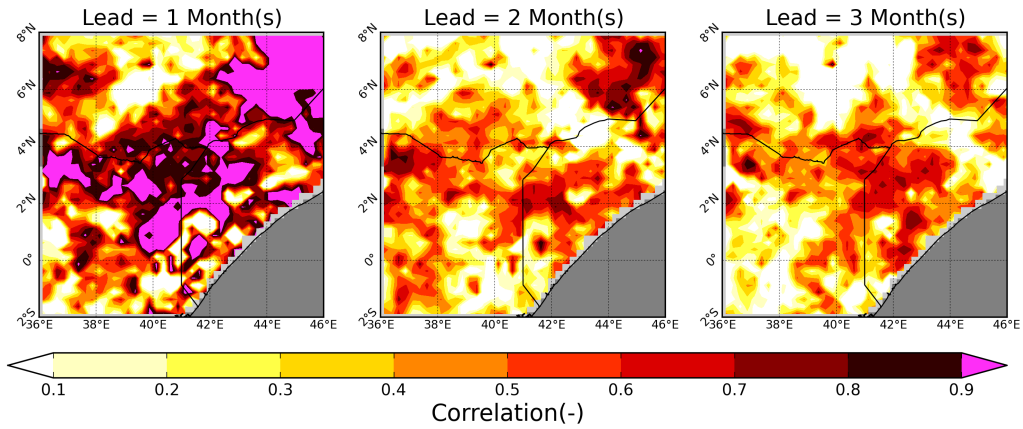
765

766 Figure 7: Comparison of ensemble median MAM precipitation forecasts and observations  
767 (CHIPRS) spatially aggregated over the focus domain.

768



**Forecast initialized on March 05**

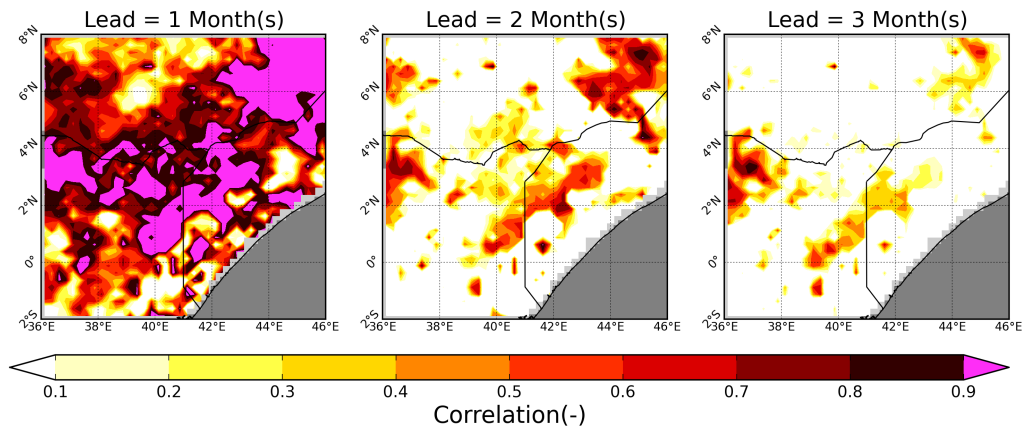


769

770

(a)

**Forecast initialized on March 05**



771

772

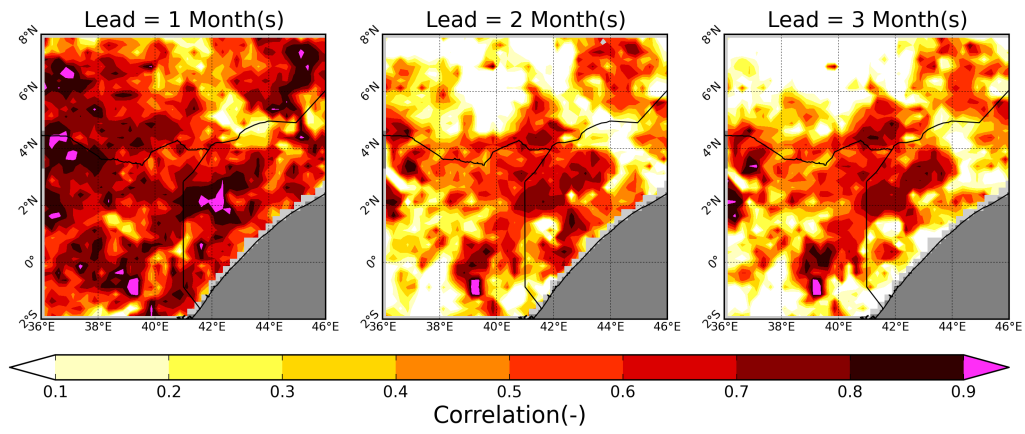
(b)

773 Figure 8: Skill of soil moisture forecasts (i.e. correlation between ensemble median of soil  
774 moisture forecasts and a posteriori estimates) initialized on March 4<sup>th</sup> (start of the season)  
775 estimated using (a) CFSv2 based seasonal climate scenarios, (b) ESP method.

776

777

### Forecast initialized on April 05

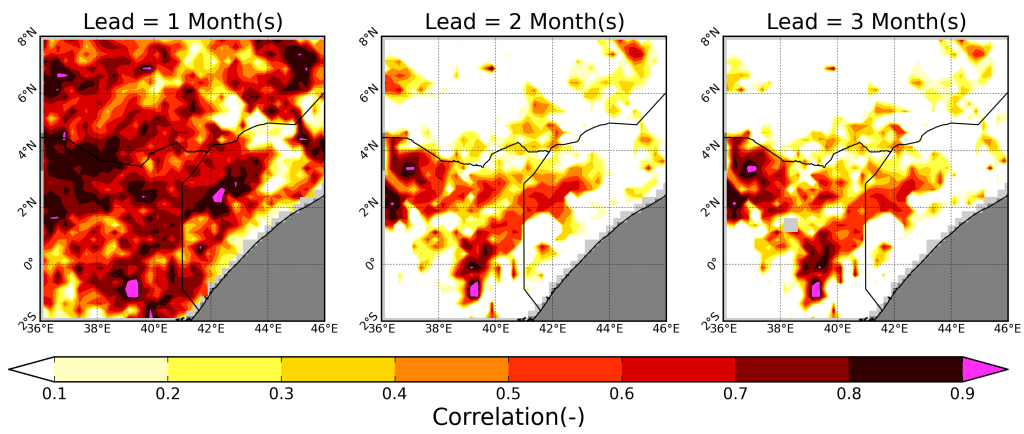


778

779

(a)

### Forecast initialized on April 05



780

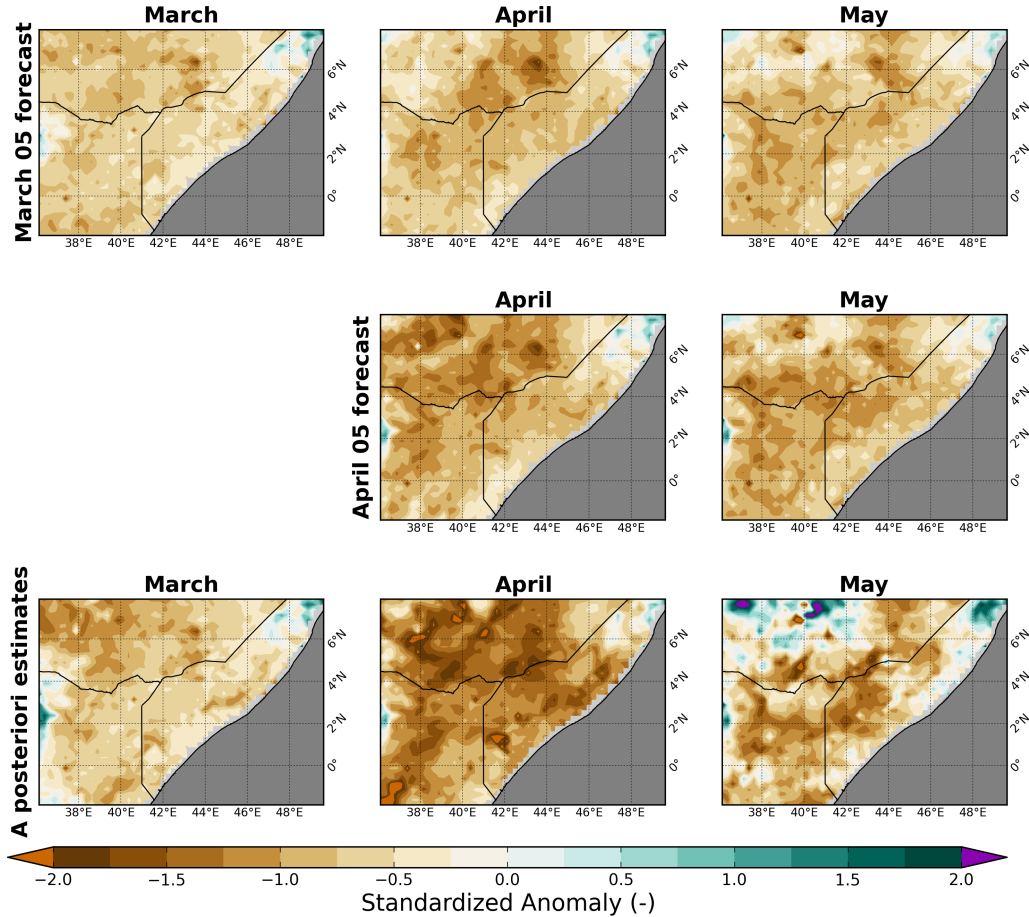
781

(b)

782 Figure 9: Same as in Fig. 8 but for forecasts initialized on April 5<sup>th</sup> (middle-of-season)

783

**Comparison of SM forecast and SM a posteriori estimates for 2011 MAM Season**

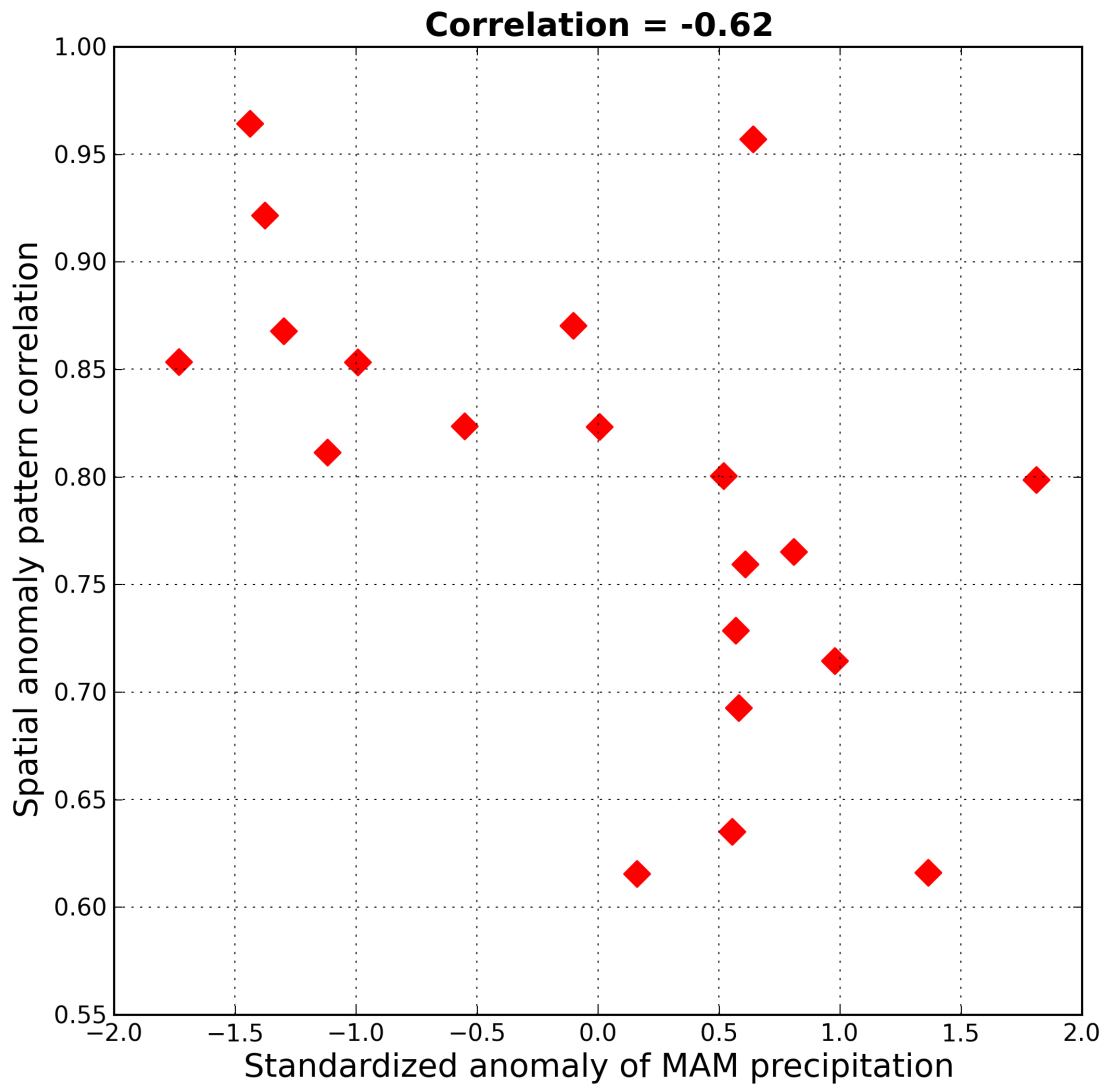


785

786 Figure 10: Comparison of standardized anomaly of SM forecast generated using CFSv2 based  
787 seasonal climate scenarios with SM a posteriori estimates during the MAM season of the year  
788 2011. Top panel shows March through May forecasts generated on March 5<sup>th</sup>, middle panel  
789 shows the same for April and May generated on April 5<sup>th</sup>, and bottom panel shows the SM a  
790 posteriori estimates.

791

792



794

795 Figure 11: Comparison between spatial anomaly pattern correlation (between MAM mean soil  
 796 moisture forecast initialized at the start of season and observation) and standardized anomaly of  
 797 MAM precipitation. This plot indicates that spatial anomaly pattern correlation is generally  
 798 higher ( $> 0.8$ ) during drought years (when standardized anomaly of MAM precipitation is  $< 0$ ).